

# Development of Rainfall Intensity-Duration-Frequency (IDF) Relationships for Siti Zone, In Case of Ethiopia Somali Regional State

Yohannes Gerezihier Gebremedhin

Lecturer, Department of Natural Resources Management, College of Agriculture and Environmental Sciences, Adigrat University, Adigrat, 50, Ethiopia

## Abstract

One of the first steps in many hydrologic design projects is determination of rainfall event. Use of inappropriate design storms could lead to malfunctions of the infrastructure systems. Hence development of IDF curves for precipitation remains a powerful tool in the risk analysis of natural hazards. Thus, this study was undertaken to develop IDF curves with their mathematical expressions in three selected rainfall stations of Ethiopian Somali region. To provide IDF information, historically observed hourly rainfall data was gathered and annual maximum data series for durations of 1, 2, 3, 6, 12 and 24 hours were extracted and fitted to different probability distribution functions for selecting best fitting distribution function to perform the frequency analysis. Extreme rainfall quantiles ( $X_T$ ) were then computed for the return periods of 2, 5, 10, 25, 50, and 100 years and taking these as an input the IDF parameters (A, B and C) were estimated with the help of MIDUSS IDF Curve fit tool software and their performance were evaluated using the regression coefficient ( $R^2$ ) and the Nash and Sutcliffe simulation efficiency ( $E_{NS}$ ). Finally, mathematical relationships were developed and IDF curves were constructed for the respective return periods of all the selected stations. Generally, the outcomes of this study indicate that Gumbel (EVI) was found to be the best fitting probability distribution in describing the given data series for all the selected stations. The IDF curve fit parameters (A, B and C) generated with the MIDUSS software shown an increasing or decreasing trend with an increase or decrease in return period and vary from 752 to 8239.3 for 'A', 0.21 to 101.49 for 'B' and 0.86 to 1.19 for parameter 'C' and parameter 'C' was found to be the most sensitive parameter. Since the R-squared and ENS values was very high, over 0.99 that depicts a strong relation between the observed and computed intensities, the developed IDF parameters can be used as a useful tool for the estimation of the rainfall design parameters.

**Keywords:** Rainfall, Intensity Duration Frequency Curve, Probability Distribution, Water resource management infrastructures, Ethiopian Somali region

## 1. INTRODUCTION

The normal balance of earth's hydrological cycle has been altered due to the changes in the temperature and precipitation patterns. Projections from climate models suggest that the probability of occurrence of intense rainfall in future will increase due to the increase in greenhouse gas emission the increase of carbon dioxide concentration in the atmosphere due to industrial activities and deforestation in the past and recent times has been identified as the major cause of global warming and climate change. Changes in earth's climate system can disrupt the delicate balance of hydrologic cycle and can eventually lead to increased occurrence of extreme events: such as flood, droughts, heat waves, summer and ice storms, etc. (Mailhot and Duchesne, 2010).

Hydrologic design of storm sewers, culverts, retention/detention basins and other components of storm water management systems are typically performed based on specified design storms derived from the rainfall intensity-duration-frequency (IDF) estimates and an assumed temporal distribution of rainfall. Use of inappropriate data or design storms could lead to malfunctions of the infrastructure systems: over-estimation may result in costly over-design or under-estimation may be associated with risk and human safety.

As one part of Ethiopia, Ethiopia Somali region is one of the vulnerable regions in the country with excessive degradation of land and highly dependent on pastoral economy and largely dominated by semi-arid climatic condition which is characterized by intensive rainfall and recurrent drought incidence. The increase in population growth, economic development and climate change have been proven by (IPCC, 2007) to cause rise in water demand, necessity of improving flood protection system and drought (water scarcity).

Flooding due to rainfall is probably the most catastrophic event among hydro meteorological hazards that cause damages to roads, municipal drainage facilities, bridges, residential, and agricultural areas in Ethiopia Somali regional state. Therefore, planning and protection of these infrastructural components, requires estimate of expected discharge from rainfall events of different magnitudes based on the current global problem of climate change. At the same time, the economic design of bridges, culverts, dams, SWC structures and other hydraulic structures demands good knowledge of the likely floods which, the structure would have to withstand during its estimated economic life in one hand, and providing strategic plans to mitigate drought incidences in the other hand are the two extreme concerning issues which has to be taken in to consideration. However,

reliable estimates of flood frequency in terms of peak flows and volumes and drought incidence remain a current challenge in hydrology. Besides this, the change in rainfall duration and frequency is one sort of challenge to hydrologists. Therefore, this study was planned with following specific objectives;

- ☞ To develop families of Intensity-Duration-Frequency curves for some of the selected stations of Ethiopia Somali Regional state for different durations and return periods
- ☞ To establish the general trends of the IDF curves
- ☞ To develop mathematical relationships of the IDF curves constructed for each selected stations

## 2. MATERIALS AND METHODES

### 2.1. Description of the Study Area

The study was conducted in Siti Zone of Dembell woreda of the Ethiopia Somali Regional State. The Ethiopia Somali Regional State geographically located, at 4<sup>0</sup> to 11<sup>0</sup> North Latitude and 40<sup>0</sup> to 48<sup>0</sup> East Longitudes. The total area of the Regional State is estimated around 325 thousand km<sup>2</sup> (MOARD-PADS, 2004).

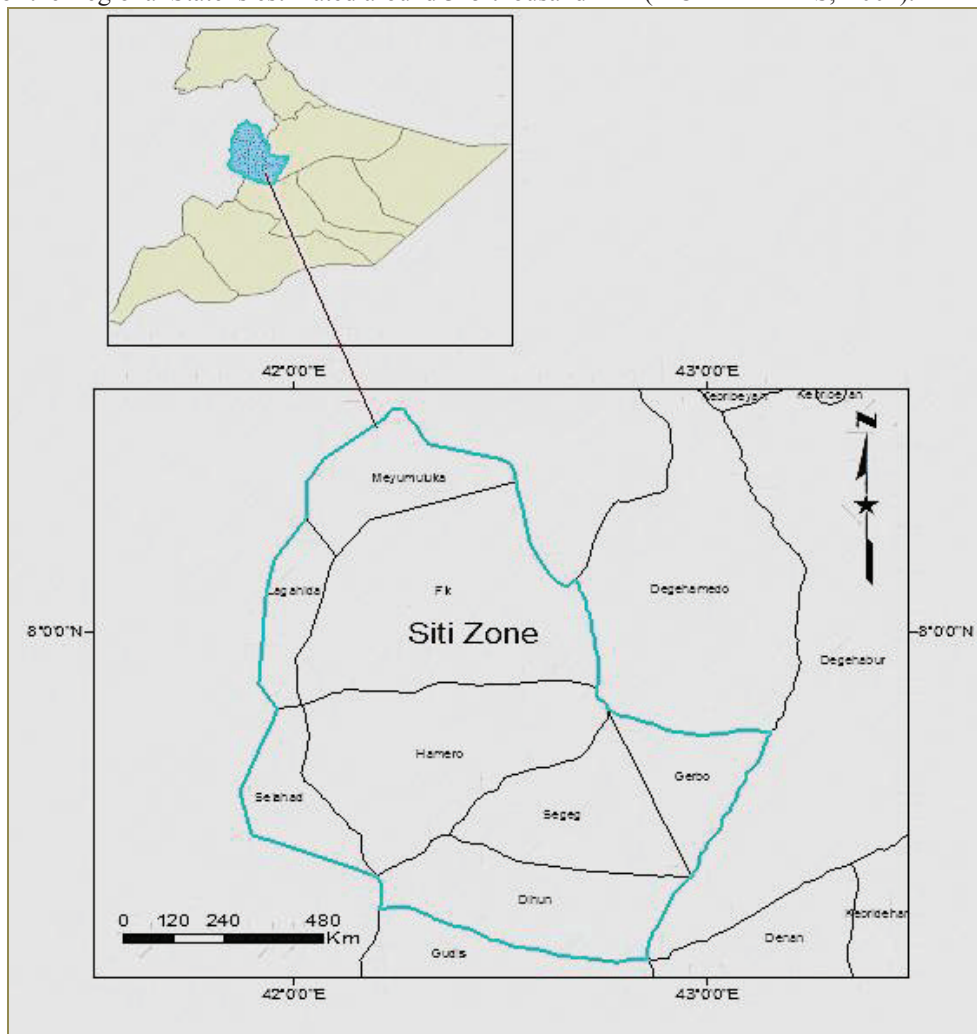


**Figure 2.** Location of Siti Zone in Ethiopia Somali regional state

**Topography:** The topography of the Somali Region is mainly lowland, however, there are some spots that are relatively high. The altitude ranges between 500 and 1,600 m.a.s.l. (MOARD-PADS, 2004).

**Climate:** The agro-ecological classification of the Zone includes A1 (arid zone one), A2 (arid zone two), SA1 (semi-arid one), and SA2 (semi-arid two). Kebribeyah is tepid to cool arid mountains and that of Babilie is tepid to cool sub-moist mountains. The environmental temperature of the area is related to altitude. At Jijiga area of higher elevation, the average monthly temperature varies between 16 to 20<sup>0</sup>C, whereas at Degahabur with lower altitude, it is about 22 to 26<sup>0</sup>C. The average annual rainfall ranged from 300 mm to 500 mm (MOARD-PADS, 2004). Within this FEZ, there are two main seasons: Gu (wet season) and Jilaal (dry season). Within the Gu there are three sub-seasons: dira' (late March to late May), Hagaana (late May to late July), and Karan (late July to late September). The Jilaal (late September to late March) can be further divided into two sub seasons: deyr (late September to late November) and kalil (late November to late March)

(MOARD-PADS, 2004).

## 2.2. Data collection

Data collected in this study consists of rainfall and geographical data. The rainfall data consisting annual totals and daily annual extreme rainfalls, and the geographical data consists GPS locations of each point gauging stations. Base map of the regional state was constructed, based on stations having annual maximum daily rainfall data set and location of each gauge collected from national weather recording agency in Addis-Ababa, Ethiopia and its branch Jigjiga weather station.

Data used in this study were recorded rainfall (predictand) which was obtained by setting selection criteria of stations to obtain a relatively better representation of the region's climatic characteristics and the regionally downscaled rainfall data (predictor) of having A1B scenario around the selected stations. Therefore, first class automatic recording stations having relatively longer record period in the region and those stations having good correlation coefficient relationship with the globally downscaled grid data (predictor) were considered to retrieve the required data for IDF development.

## 2.3. Data pre- processing

**Checking data quality (Homogeneity test);** the homogeneity of all the series was checked by a non-parametric Mann-kendall rank test at 5% significance level.

**Consistency analysis of the data set;** any inconsistency in the data set was checked and corrected using double mass-curve method.

**Missing value estimation;** rainfall data often has significant portion of the historic record missing needs to be estimated. For this study, the Inverse Distance Weighting method was used for interpolation of rainfall data. This method is widely used, and recommended by the United States Army Corps of Engineers (USACE, 2000).

## 2.4. Formulation of Climate change Scenarios

Climate change scenarios are obtained as outputs of global circulation model (AOGCM) simulations and do not represent future predictions or forecasts, but simply offer possibilities of what might happen if the future development follows a certain course of action i.e., continual growth of population, increased carbon dioxide emissions, increased urbanization, etc. ( Nakicenovic and Swart, 2000).

In this work, the climate change scenario data was obtained from the Canadian Climate Impacts Scenarios group at the University of Victoria, Canada (<http://www.cics.uvic.ca>). and down scaled to the station data using the SDSM 4.2 software which is a decision support tool for assessing local climate change impacts using a robust statistical down scaling technique.

SDSM 4.2 (Statistical Down Scaling Model) facilitates the rapid development of multiple, low cost, single site scenarios of daily surface weather variables under present and future climate forcing. Additionally, the software performs ancillary tasks of data quality control and transformation, predictor variable prescreening, automatic model calibration, basic diagnostic testing, statistical analyses and graphing of climate data. The SDSM software reduces the task of statistically downscaling daily weather series into seven discrete steps:

- ☞ quality control and data transformation
- ☞ screening of predictor variables
- ☞ model calibration
- ☞ weather generation (using observed predictors)
- ☞ statistical analyses
- ☞ graphing model output
- ☞ Scenario generation (using climate model predictors)

Time series data was extracted for the grid point containing the Region, for a particular time slice. For this study, the time slice of 2040-2069 and 2070-2099 was used for all climate change scenarios, thus representing average climatic conditions for the year 2050s and 2080s respectively. Historic global circulation data, also taken from the University of Victoria, represents the baseline global data.

## 2.5. Disaggregation of Daily Rainfall

The Hyetos software disaggregates the daily rainfall at a single site into hourly data using Bartlett Lewis model as a background stochastic model for rainfall generation. The daily series was divided into clusters of wet days and several runs from the Bartlett Lewis model were performed separately for each cluster of wet days. The runs continue until the sequence of synthetic daily depths matches the sequence of daily totals with a tolerance distance, defined as: Observed hourly data was used as a template on how the hourly values of the generated outputs would look like. A specific number of days were considered to compare with the present day value. (Mansour and Burn, 2010) determine the best match:

$$z_i = \sqrt{(w_1 * (y_i - x_i)^2) + (w_2 * (e_y - e_x)^2)} \quad (2.1)$$

Where,  $y_i$  is the daily rainfall output from weather generator,  $x_i$  is the historical observed daily rainfall,  $e_y$  and  $e_x$  are the events calculated from WG outputs and historical observed data respectively. The weights  $w_1$  and  $w_2$  are used to identify the best historical hourly ratio of the data.

## 2.6. Model Performance Testing

In order to test the output of the weather-generating model a number of different statistical tools can be employed. Box and whisker plot method were used for this study to show the comparison between generated and observed data. Three types of plots, including monthly totals, auto and cross-correlations were applied. In this regard, the plot showing monthly totals is in the manner where the horizontal axis shows the month of year, while the vertical axis displays the monthly total. The second type of a box and whisker plot is the way where autocorrelation of data was presented. Autocorrelation is a statistical tool used to test the correlation of a time series with a lagged version of itself for identifying patterns of randomness. It is also used to identify a temporal character of generated data. Mathematically, it is defined as:

$$autocorr = \frac{1}{(n-k)\sigma^2} \sum_{i=1}^{n-k} (x_i - \bar{x})(x_{i+k} - \bar{x}) \quad (2.2)$$

Where  $k$  is the time lag,  $x_i$  is the data value,  $\bar{x}$  the mean and  $\sigma^2$  is the variance of the data.

Autocorrelation takes on values between [-1, +1]. Values of zero indicate perfectly random data (i.e., no correlation), while non-zero values indicate a degree of correlation, or non-randomness. A high negative value indicates a high degree of correlation, but of the inverse of the series.

Cross-correlation compares two time series signals to each other. This is one way of testing spatial characteristics of generated data between two different locations. Cross-correlation is therefore a statistical tool used to compare correlations between two signals (such as rainfall between two stations). Its mathematical form:

$$crosscorr = \frac{\sum_{i=1}^{n-k} (x_i - \bar{x})(y_{i+k} - \bar{y})}{\sum_{i=1}^{n-k} (x_i - \bar{x})^2 (y_{i+k} - \bar{y})^{-1/2}} \quad (2.3)$$

Where  $x_i$  and  $y_i$  are two time series to be compared. The range of cross-correlation values is between [-1, +1], with zero indicating no correlation, while its bounds show maximum correlation.

The extent of the generated data displayed with box and whisker plots has to be shown on a monthly time scale. This means that the weather generator output should be aggregated to a monthly time step in case when generated monthly totals were contrasted with totals historically observed. Auto and cross-correlations were computed on a daily time step, and then averaged on a monthly basis for presentation using box and whisker plots.

## 2.7. Intensity-Duration-Frequency Analysis

The intensity duration frequency analysis starts by gathering time series records of different durations. After time series data was gathered, annual extremes were extracted from records for duration's data. The annual extreme data was then fit to a probability distribution in order to estimate rainfall quantities. The fit of the probability distribution is necessary in order to standardize the character of rainfall across stations with widely varying lengths of record.

### 2.7.1. Fitting the probability Distribution

For Ethiopia, Gumbel's extreme value distribution is recommended to fit the annual extremes rainfall data (Asres, 2008). However, the data series for every station was also tested for other distributions to select the best distribution function. The Gumbel probability distribution has the following form (Watt *et al.*, 1989):

$$x_t = \mu_z + k_T \delta_z \quad (2.4)$$

Where,  $x_t$  represents the magnitude of the  $T$ -year event,  $\mu_z$  and  $\delta_z$  are the mean and standard deviation of the annual maximum series, and  $k_T$  is a frequency factor depending on the return period,  $T$ . The frequency factor  $k_T$  was obtained using the relationship:

$$k_T = \frac{-\sqrt{6}}{\pi} \left| 0.5772 + \ln \left( \ln \left( \frac{T}{T+1} \right) \right) \right| \quad (2.5)$$

The above method can be employed to calculate rainfall frequency for durations of 5, 10, 30 minutes and 1, 2, 6, 12 and 24 hours (MSC). However, for the stations do not have observed sub-hourly data, the calculation of the frequencies for periods shorter than 1 hour can be based on the ratios provided by the World Meteorological Organization (MTO, 1997):

Duration (min)	5	10	15	30
Ratio (n-min to 60-min)	0.29	0.45	0.57	0.79

The IDF data derived with above method is typically fitted to a continuous function in order to make the process of IDF data interpolation more efficient i.e. if the ratio of any duration is not available, the IDF data is fitted to the following three-parameter function:

$$i = \frac{A}{(t_d + B)^C} \quad (2.6)$$

Where  $i$  is the rainfall intensity (mm/hr),  $d_t$  the rainfall duration (min), and  $A$ ,  $B$ , and  $C$  are coefficients. After selecting a reasonable value of parameter  $B$ , method of least square was used to estimate values of  $A$  and  $C$ . The calculation is repeated for a number of different values of  $B$  in order to achieve the closest possible fit of the data (MTO, 1997). After IDF data was fitted to the above function, plots of rainfall intensity vs. duration (for each return period) produced.

### 2.7.2. Testing the Goodness of Fit of Data

The chi-square goodness of fit test was used for the generated annual maximum rainfall value of all durations and stations to see whether the selected probability distribution fit the theoretical frequency distribution.

### 2.7.3. Computation of Extreme Value

The rainfall events  $X_T$  (mm) exceeding the observed value was estimated numerically using the following formula:

$$y_T = \bar{y} + K_T S_y \longrightarrow X_T = \text{antilog}(\bar{y} + K_T S_y) \quad (2.7)$$

### 2.7.4. Estimation of IDF Curve Coefficients

The extrem rainfall value ( $X_T$ ) or the intensity values ( $I$ ) was used to estimate the IDF curve coefficients ( $a$ ,  $b$  and  $c$ ) using the IDF Curve Fit software known as MIDUSS which operates using either depth of rainfall ( $X_T$ ) or rainfall intensity ( $I$ ) data in either metric or U.S. customary units and displays a comparison between the observed and computed data in tabular form.

### 2.7.5. Comparison of IDF Results

Updated IDF curves for respective climate change scenarios (rainfall intensity) were compared with the present IDF curves of the respective stations as well as between themselves. Relative difference between the curves was determined using the following relationship:

$$RD = \frac{|x_1 - x_2|}{\left(\frac{x_1 + x_2}{2}\right)} * 100 \quad (2.8)$$

The purpose of comparison results is to indicate that whether the rainfall magnitude was increase or decrease under climate change for all durations and return periods of the respective stations (Slobodan P. Simonovic and Angela Peck, 2010).

### 2.7.6. Construction of IDF Curves

Finally, information was summarized by plotting the IDF curve on a log-log graph paper, the durations on the horizontal axis, the rate of rainfall (intensity in depth per unit of time) on the vertical axis and the curves for each return period.

## 3. RESULTS AND DISCUSSION

In this section, the comparison of different probability distributions (such as Gumbel EVI, Log-normal and Log-Pearson) and the selection of best fitting probability distribution functions, the result of the test of the selected probability distribution functions and values of extreme rainfall quantiles are presented and described. In addition, estimation of IDF parameters, testing of the parameters performance, sensitivity of the parameters and development of IDF curves and formulation of their mathematical expressions are presented and discussed.

### 3.1. Comparison of the Probability Distribution Functions

For the purpose of comparison, the ranked annual maximum rainfall data sets of selected durations of 1, 2, 3, 6, 12, and 24 hours were fitted to Gumbel EVI, Log-normal and Log-Pearson Type III frequency distributions and plots of annual maximum rainfall against these distributions were made. Finally, R-squared values were determined.

**Table 1.** Maximum rainfall and reduced variate (Yt) for EVI probability distribution of Lefe-isa station

Duration (hr)						Rank (m)	P=m/n+1	T=1/P	T/(T-1)	ln	Yt =neg ln(ln)
1	2	3	6	12	24						
59.1	62.0	62.0	62.0	62.0	62.0	1	0.06	17.00	1.06	0.06	2.80
51.6	51.6	56.4	56.7	56.7	56.7	2	0.12	8.50	1.13	0.13	2.08
33.4	33.4	36.1	37.2	45.5	47.0	3	0.18	5.67	1.21	0.19	1.64
28.0	33.1	33.4	35.9	44.7	45.6	4	0.24	4.25	1.31	0.27	1.32
27.0	29.8	33.1	33.1	36.9	45.0	5	0.29	3.40	1.42	0.35	1.05
26.7	27.0	31.2	31.3	36.5	38.1	6	0.35	2.83	1.55	0.44	0.83
22.5	23.4	23.4	31.2	35.3	36.5	7	0.41	2.43	1.70	0.53	0.63
22.4	22.4	22.4	26.4	33.8	35.3	8	0.47	2.13	1.89	0.64	0.45
20.2	20.2	21.6	23.2	32.4	34.0	9	0.53	1.89	2.13	0.75	0.28
19.8	19.8	21.2	21.9	26.7	33.7	10	0.59	1.70	2.43	0.89	0.12
18.6	19.5	19.8	21.6	26.4	31.5	11	0.65	1.55	2.83	1.04	-0.04
14.5	19.2	19.2	21.5	24.6	28.0	12	0.71	1.42	3.40	1.22	-0.20
14.1	18.1	18.4	19.8	22.8	26.7	13	0.76	1.31	4.25	1.45	-0.37
12.4	15.5	15.5	19.3	19.8	19.8	14	0.82	1.21	5.67	1.73	-0.55
11.2	12.4	12.7	18.8	19.3	19.3	15	0.88	1.13	8.50	2.14	-0.76
8.5	12.3	12.6	16.4	17.3	19.2	16	0.94	1.06	17.00	2.83	-1.04
24.4	26.2	27.4	29.8	33.8	36.1	Mean					
13.9	13.7	14	13.3	13	12.7	SD					

**Table 2.** Maximum rainfall and standard normal variable (Z) for log normal probability distribution of Lefe-isa station

Duration(hr)						Rank (m)	P	T	1/p*p	ln	W	W <sub>2</sub>	W <sub>3</sub>	A	B	A/B	KT
1	2	3	6	12	24												
59.1	62.0	62.0	62.0	62.0	62.0	1	0.04	26.00	676.00	6.52	2.55	6.52	16.63	4.63	5.91	0.78	1.77
51.6	51.6	56.4	56.7	56.7	56.7	2	0.10	10.00	100.00	4.61	2.15	4.61	9.88	4.29	4.96	0.86	1.28
33.4	33.4	36.1	37.2	45.5	47.0	3	0.16	6.19	38.32	3.65	1.91	3.65	6.96	4.09	4.44	0.92	0.99
28.0	33.1	33.4	35.9	44.7	45.6	4	0.22	4.48	20.10	3.00	1.73	3.00	5.20	3.94	4.06	0.97	0.76
27.0	29.8	33.1	33.1	36.9	45.0	5	0.28	3.51	12.34	2.51	1.59	2.51	3.98	3.81	3.75	1.02	0.57
26.7	27.0	31.2	31.3	36.5	38.1	6	0.35	2.89	8.35	2.12	1.46	2.12	3.09	3.71	3.49	1.06	0.40
22.5	23.4	23.4	31.2	35.3	36.5	7	0.41	2.45	6.02	1.79	1.34	1.79	2.40	3.61	3.26	1.11	0.23
22.4	22.4	22.4	26.4	33.8	35.3	8	0.47	2.13	4.54	1.51	1.23	1.51	1.86	3.52	3.05	1.15	0.08
20.2	20.2	21.6	23.2	32.4	34.0	9	0.53	1.88	4.54	1.51	1.23	1.51	1.86	3.52	3.05	1.15	-0.08
19.8	19.8	21.2	21.9	26.7	33.7	10	0.59	1.69	6.02	1.79	1.34	1.79	2.40	3.61	3.26	1.11	-0.23
18.6	19.5	19.8	21.6	26.4	31.5	11	0.65	1.53	8.35	2.12	1.46	2.12	3.09	3.71	3.49	1.06	-0.40
14.5	19.2	19.2	21.5	24.6	28.0	12	0.72	1.40	12.34	2.51	1.59	2.51	3.98	3.81	3.75	1.02	-0.57
14.1	18.1	18.4	19.8	22.8	26.7	13	0.78	1.29	20.10	3.00	1.73	3.00	5.20	3.94	4.06	0.97	-0.76
12.4	15.5	15.5	19.3	19.8	19.8	14	0.84	1.19	38.32	3.65	1.91	3.65	6.96	4.09	4.44	0.92	-0.99
11.2	12.4	12.7	18.8	19.3	19.3	15	0.90	1.11	100.00	4.61	2.15	4.61	9.88	4.29	4.96	0.86	-1.28
8.5	12.3	12.6	16.4	17.3	19.2	16	0.96	1.04	676.00	6.52	2.55	6.52	16.63	4.63	5.91	0.78	-1.77

**Table 3.** Maximum rainfall and pearson frequency factor (KT) for log pearson probability distribution of Lefe-isa station

Duration(hr)						Rank	P	W	Z	KT <sub>1</sub>	KT <sub>2</sub>	KT <sub>3</sub>	KT <sub>6</sub>	KT <sub>12</sub>	KT <sub>24</sub>
1	2	3	6	12	24										
59.1	62.0	62.0	62.0	62.0	62.0	1	0.03	2.63	1.86	1.93	2.01	1.99	2.05	1.90	1.81
51.6	51.6	56.4	56.7	56.7	56.7	2	0.09	2.18	1.32	1.34	1.36	1.35	1.36	1.33	1.30
33.4	33.4	36.1	37.2	45.5	47.0	3	0.16	1.93	1.01	1.01	1.00	1.01	1.00	1.01	1.01
28.0	33.1	33.4	35.9	44.7	45.6	4	0.22	1.74	0.78	0.76	0.74	0.75	0.73	0.77	0.78
27.0	29.8	33.1	33.1	36.9	45.0	5	0.28	1.59	0.58	0.56	0.53	0.54	0.52	0.57	0.59
26.7	27.0	31.2	31.3	36.5	38.1	6	0.34	1.46	0.40	0.38	0.35	0.35	0.33	0.39	0.42
22.5	23.4	23.4	31.2	35.3	36.5	7	0.41	1.34	0.24	0.21	0.17	0.18	0.16	0.22	0.26
22.4	22.4	22.4	26.4	33.8	35.3	8	0.47	1.23	0.08	0.05	0.01	0.02	0.00	0.06	0.10
20.2	20.2	21.6	23.2	32.4	34.0	9	0.53	1.23	-0.08	-0.11	-0.14	-0.13	-0.16	-0.09	-0.06
19.8	19.8	21.2	21.9	26.7	33.7	10	0.59	1.34	-0.24	-0.26	-0.29	-0.29	-0.31	-0.25	-0.22
18.6	19.5	19.8	21.6	26.4	31.5	11	0.66	1.46	-0.40	-0.43	-0.45	-0.44	-0.46	-0.41	-0.38
14.5	19.2	19.2	21.5	24.6	28.0	12	0.72	1.59	-0.58	-0.60	-0.62	-0.61	-0.62	-0.59	-0.56
14.1	18.1	18.4	19.8	22.8	26.7	13	0.78	1.74	-0.78	-0.79	-0.79	-0.79	-0.80	-0.78	-0.77
12.4	15.5	15.5	19.3	19.8	19.8	14	0.84	1.93	-1.01	-1.01	-1.00	-1.00	-1.00	-1.01	-1.01
11.2	12.4	12.7	18.8	19.3	19.3	15	0.91	2.18	-1.32	-1.30	-1.26	-1.27	-1.25	-1.31	-1.33
8.5	12.3	12.6	16.4	17.3	19.2	16	0.97	2.63	-1.86	-1.79	-1.70	-1.72	-1.66	-1.82	-1.92

**Table 4.** Maximum rainfall and reduced variate (Yt) for EVI probability distribution of Chinaksa station

Duration(hr)						Rank					Yt=
1	2	3	6	12	24	(m)	$P=m/n+1$	$T=1/P$	$T/(T-1)$	ln	neg ln(ln)
63.9	68.7	89.4	93.9	93.9	93.9	1	1.10	0.10	2.35	0.06	2.80
40.0	68.2	80.3	80.3	80.3	80.3	2	1.22	0.20	1.61	0.13	2.08
40.0	64.1	69.8	70.1	71.9	72.7	3	1.38	0.32	1.14	0.19	1.64
30.0	39.8	69.2	69.8	69.8	71.0	4	1.57	0.45	0.79	0.27	1.32
26.4	36.0	36.0	43.0	46.9	50.5	5	1.83	0.61	0.50	0.35	1.05
21.6	33.9	33.9	36.8	44.0	50.0	6	2.20	0.79	0.24	0.44	0.83
10.7	15.9	20.9	23.9	36.6	41.0	7	2.75	1.01	-0.01	0.53	0.63
8.4	8.4	8.4	9.2	9.2	12.9	8	3.67	1.30	-0.26	0.64	0.45
4.5	7.6	7.6	8.9	8.9	9.2	9	5.50	1.70	-0.53	0.75	0.28
4.3	5.9	6.9	8.4	8.4	9.2	10	11.00	2.40	-0.87	0.89	0.12
25.0	34.8	42.2	44.4	47.0	49.1	Mean					
19.24	25.3	32.2	32.2	31.5	30.88	SD					

**Table 5.** Maximum rainfall and standard normal variable (Z) for log normal probability distribution of Chinaksa station

Duration(hr)						Rank	P	T	1/p*p	ln	W	KT=Z
1	2	3	6	12	24							
63.9	68.7	89.4	93.9	93.9	93.9	1	0.06	16.40	268.96	5.59	2.37	1.55
40.0	68.2	80.3	80.3	80.3	80.3	2	0.16	6.31	39.79	3.68	1.92	1.00
40.0	64.1	69.8	70.1	71.9	72.7	3	0.26	3.90	15.25	2.72	1.65	0.66
30.0	39.8	69.2	69.8	69.8	71.0	4	0.35	2.83	8.00	2.08	1.44	0.37
26.4	36.0	36.0	43.0	46.9	50.5	5	0.45	2.22	4.91	1.59	1.26	0.12
21.6	33.9	33.9	36.8	44.0	50.0	6	0.55	1.82	4.91	1.59	1.26	-0.12
10.7	15.9	20.9	23.9	36.6	41.0	7	0.65	1.55	8.00	2.08	1.44	-0.37
8.4	8.4	8.4	9.2	9.2	12.9	8	0.74	1.34	15.25	2.72	1.65	-0.66
4.5	7.6	7.6	8.9	8.9	9.2	9	0.84	1.19	39.79	3.68	1.92	-1.00
4.3	5.9	6.9	8.4	8.4	9.2	10	0.94	1.06	268.96	5.59	2.37	-1.55

**Table 6.** Maximum rainfall and pearson frequency factor (KT) for Log pearson probability distribution of Chinaksa station

Duration(hr)						Rank (m)	P	W	Z	KT <sub>1</sub>	KT <sub>2</sub>	KT <sub>3</sub>	KT <sub>6</sub>	KT <sub>12</sub>	KT <sub>24</sub>
1	2	3	6	12	24										
63.9	68.7	89.4	93.9	93.9	93.9	1	0.05	2.45	1.65	1.51	1.51	1.60	1.49	1.39	1.35
40.0	68.2	80.3	80.3	80.3	80.3	2	0.15	1.95	1.04	1.02	1.02	1.03	1.02	1.00	0.99
40.0	64.1	69.8	70.1	71.9	72.7	3	0.25	1.67	0.67	0.71	0.71	0.69	0.71	0.73	0.74
30.0	39.8	69.2	69.8	69.8	71.0	4	0.35	1.45	0.38	0.44	0.45	0.41	0.45	0.49	0.50
26.4	36.0	36.0	43.0	46.9	50.5	5	0.45	1.26	0.13	0.20	0.20	0.15	0.21	0.25	0.27
21.6	33.9	33.9	36.8	44.0	50.0	6	0.55	1.26	-0.13	-0.05	-0.05	-0.10	-0.04	0.01	0.03
10.7	15.9	20.9	23.9	36.6	41.0	7	0.65	1.45	-0.38	-0.32	-0.32	-0.36	-0.31	-0.26	-0.24
8.4	8.4	8.4	9.2	9.2	12.9	8	0.75	1.67	-0.67	-0.63	-0.63	-0.66	-0.62	-0.58	-0.57
4.5	7.6	7.6	8.9	8.9	9.2	9	0.85	1.95	-1.04	-1.03	-1.03	-1.04	-1.03	-1.02	-1.02
4.3	5.9	6.9	8.4	8.4	9.2	10	0.95	2.45	-1.65	-1.76	-1.77	-1.69	-1.78	-1.85	-1.87

**Table 7.** Maximum rainfall and reduced variate (Yt) for EVI probability distribution of Jigjiga station

Duration(hr)						Rank (m)	P	T	1/T	Ln	YT
1	2	3	6	12	24						
84.8	114.3	114.6	114.7	115.0	115.0	1	0.03	32.00	1.03	0.03	3.45
61.2	61.2	61.2	61.2	61.9	62.0	2	0.06	16.00	1.07	0.06	2.74
49.7	54.2	54.2	54.2	61.2	61.9	3	0.09	10.67	1.10	0.10	2.32
49.1	49.7	49.7	52.5	58.2	61.2	4	0.13	8.00	1.14	0.13	2.01
45.1	49.3	49.3	50.5	54.2	59.0	5	0.16	6.40	1.19	0.17	1.77
38.5	48.4	48.4	49.7	53.6	54.9	6	0.19	5.33	1.23	0.21	1.57
38.4	46.8	46.8	47.2	53.2	54.2	7	0.22	4.57	1.28	0.25	1.40
38.1	41.7	43.1	43.7	50.4	54.2	8	0.25	4.00	1.33	0.29	1.25
38.0	40.9	41.7	43.0	49.1	53.2	9	0.28	3.56	1.39	0.33	1.11
37.7	40.3	40.3	42.7	47.2	50.8	10	0.31	3.20	1.45	0.37	0.98
37.5	39.7	39.7	42.0	46.4	47.2	11	0.34	2.91	1.52	0.42	0.86
35.2	38.1	38.1	41.7	43.5	46.4	12	0.38	2.67	1.60	0.47	0.76
32.1	38.0	38.0	41.3	43.0	45.0	13	0.41	2.46	1.68	0.52	0.65
30.4	36.7	36.7	40.4	42.0	43.5	14	0.44	2.29	1.78	0.58	0.55
29.4	35.9	36.4	38.0	41.4	43.0	15	0.47	2.13	1.88	0.63	0.46
29.1	35.2	36.3	37.9	40.4	42.0	16	0.50	2.00	2.00	0.69	0.37
27.2	33.2	36.2	36.7	40.0	41.8	17	0.53	1.88	2.13	0.76	0.28
27.0	32.9	35.2	36.4	39.5	40.4	18	0.56	1.78	2.29	0.83	0.19
25.8	32.6	32.9	36.3	38.0	40.1	19	0.59	1.68	2.46	0.90	0.10
25.0	30.9	32.6	36.2	37.9	40.0	20	0.63	1.60	2.67	0.98	0.02
24.6	30.4	32.3	34.3	36.6	39.9	21	0.66	1.52	2.91	1.07	-0.07
23.4	30.0	30.4	34.0	36.3	36.6	22	0.69	1.45	3.20	1.16	-0.15
23.1	29.6	30.1	32.3	36.2	36.3	23	0.72	1.39	3.56	1.27	-0.24
21.7	29.4	30.0	31.3	34.8	36.2	24	0.75	1.33	4.00	1.39	-0.33
21.2	28.8	29.4	30.8	34.0	34.0	25	0.78	1.28	4.57	1.52	-0.42
21.2	25.0	28.8	30.4	31.3	31.3	26	0.81	1.23	5.33	1.67	-0.52
19.1	24.0	27.6	29.4	30.4	30.4	27	0.84	1.19	6.40	1.86	-0.62
17.5	22.7	25.0	26.4	29.4	30.4	28	0.88	1.14	8.00	2.08	-0.73
17.0	21.3	23.2	25.5	27.5	30.2	29	0.91	1.10	10.67	2.37	-0.86
15.7	17.0	21.3	23.6	26.7	27.5	30	0.94	1.07	16.00	2.77	-1.02
15.0	15.7	15.7	23.2	26.2	26.7	31	0.97	1.03	32.00	3.47	-1.24
32.2	37.9	38.9	40.9	44.0	45.7	Mean					
14.73	17.7	17.19	16.49	16.5	16.57	SD					



**Table 8.** Maximum rainfall and standard normal variable (Z) log normal probability distribution of Jigjiga station

Duration (hr)						Rank (m)	P	T	ln	W	KT=Z
1	2	3	6	12	24						
84.8	114.3	114.6	114.7	115.0	115.0	1	0.02	50.00	7.82	2.80	2.42
61.2	61.2	61.2	61.2	61.9	62.0	2	0.05	19.23	5.91	2.43	1.98
49.7	54.2	54.2	54.2	61.2	61.9	3	0.08	11.90	4.95	2.23	1.72
49.1	49.7	49.7	52.5	58.2	61.2	4	0.12	8.62	4.31	2.08	1.52
45.1	49.3	49.3	50.5	54.2	59.0	5	0.15	6.76	3.82	1.95	1.35
38.5	48.4	48.4	49.7	53.6	54.9	6	0.18	5.56	3.43	1.85	1.21
38.4	46.8	46.8	47.2	53.2	54.2	7	0.21	4.72	3.10	1.76	1.08
38.1	41.7	43.1	43.7	50.4	54.2	8	0.24	4.10	2.82	1.68	0.95
38.0	40.9	41.7	43.0	49.1	53.2	9	0.28	3.62	2.57	1.60	0.84
37.7	40.3	40.3	42.7	47.2	50.8	10	0.31	3.25	2.36	1.53	0.73
37.5	39.7	39.7	42.0	46.4	47.2	11	0.34	2.94	2.16	1.47	0.62
35.2	38.1	38.1	41.7	43.5	46.4	12	0.37	2.69	1.98	1.41	0.51
32.1	38.0	38.0	41.3	43.0	45.0	13	0.40	2.48	1.81	1.35	0.41
30.4	36.7	36.7	40.4	42.0	43.5	14	0.44	2.29	1.66	1.29	0.30
29.4	35.9	36.4	38.0	41.4	43.0	15	0.47	2.14	1.52	1.23	0.20
29.1	35.2	36.3	37.9	40.4	42.0	16	0.50	2.00	1.39	1.18	0.10
27.2	33.2	36.2	36.7	40.0	41.8	17	0.53	1.88	1.52	1.23	-0.20
27.0	32.9	35.2	36.4	39.5	40.4	18	0.56	1.77	1.66	1.29	-0.30
25.8	32.6	32.9	36.3	38.0	40.1	19	0.60	1.68	1.81	1.35	-0.41
25.0	30.9	32.6	36.2	37.9	40.0	20	0.63	1.59	1.98	1.41	-0.51
24.6	30.4	32.3	34.3	36.6	39.9	21	0.66	1.52	2.16	1.47	-0.62
23.4	30.0	30.4	34.0	36.3	36.6	22	0.69	1.45	2.36	1.53	-0.73
23.1	29.6	30.1	32.3	36.2	36.3	23	0.72	1.38	2.57	1.60	-0.84
21.7	29.4	30.0	31.3	34.8	36.2	24	0.76	1.32	2.82	1.68	-0.95
21.2	28.8	29.4	30.8	34.0	34.0	25	0.79	1.27	3.10	1.76	-1.08
21.2	25.0	28.8	30.4	31.3	31.3	26	0.82	1.22	3.43	1.85	-1.21
19.1	24.0	27.6	29.4	30.4	30.4	27	0.85	1.17	3.82	1.95	-1.35
17.5	22.7	25.0	26.4	29.4	30.4	28	0.88	1.13	4.31	2.08	-1.52
17.0	21.3	23.2	25.5	27.5	30.2	29	0.92	1.09	4.95	2.23	-1.72
15.7	17.0	21.3	23.6	26.7	27.5	30	0.95	1.05	5.91	2.43	-1.98
15.0	15.7	15.7	23.2	26.2	26.7	31	0.98	1.02	7.82	2.80	-2.42

**Table 9.** Maximum rainfall and pearson frequency factor (KT) for Log pearson probability distribution of Jigjiga station

Duration(hr)						Rank (m)	P	W	Z	KT1	KT2	KT3	KT6	KT12	KT24
1	2	3	6	12	24										
84.8	114.3	114.6	114.7	115.0	115.0	1	0.02	2.87	2.12	2.36	2.39	2.46	2.64	2.60	2.54
61.2	61.2	61.2	61.2	61.9	62.0	2	0.05	2.46	1.65	1.76	1.78	1.80	1.86	1.85	1.83
49.7	54.2	54.2	54.2	61.2	61.9	3	0.08	2.24	1.39	1.45	1.46	1.47	1.47	1.47	1.47
49.1	49.7	49.7	52.5	58.2	61.2	4	0.11	2.09	1.21	1.23	1.23	1.23	1.21	1.22	1.22
45.1	49.3	49.3	50.5	54.2	59.0	5	0.15	1.96	1.05	1.05	1.05	1.04	1.00	1.02	1.03
38.5	48.4	48.4	49.7	53.6	54.9	6	0.18	1.86	0.92	0.90	0.90	0.89	0.84	0.85	0.87
38.4	46.8	46.8	47.2	53.2	54.2	7	0.21	1.77	0.80	0.77	0.76	0.75	0.69	0.71	0.73
38.1	41.7	43.1	43.7	50.4	54.2	8	0.24	1.68	0.70	0.65	0.65	0.63	0.57	0.58	0.60
38.0	40.9	41.7	43.0	49.1	53.2	9	0.27	1.61	0.60	0.54	0.54	0.52	0.45	0.47	0.49
37.7	40.3	40.3	42.7	47.2	50.8	10	0.31	1.54	0.50	0.44	0.44	0.41	0.35	0.37	0.39
37.5	39.7	39.7	42.0	46.4	47.2	11	0.34	1.47	0.41	0.35	0.34	0.32	0.25	0.27	0.29
35.2	38.1	38.1	41.7	43.5	46.4	12	0.37	1.41	0.33	0.26	0.25	0.23	0.16	0.18	0.20
32.1	38.0	38.0	41.3	43.0	45.0	13	0.40	1.35	0.24	0.17	0.16	0.14	0.08	0.09	0.11
30.4	36.7	36.7	40.4	42.0	43.5	14	0.44	1.29	0.16	0.09	0.08	0.06	-0.01	0.01	0.03
29.4	35.9	36.4	38.0	41.4	43.0	15	0.47	1.23	0.08	0.01	0.00	-0.02	-0.08	-0.07	-0.05
29.1	35.2	36.3	37.9	40.4	42.0	16	0.50	1.18	0.00	-0.07	-0.08	-0.10	-0.16	-0.15	-0.13
27.2	33.2	36.2	36.7	40.0	41.8	17	0.53	1.23	-0.08	-0.15	-0.16	-0.18	-0.23	-0.22	-0.20
27.0	32.9	35.2	36.4	39.5	40.4	18	0.56	1.29	-0.16	-0.23	-0.24	-0.26	-0.30	-0.29	-0.28
25.8	32.6	32.9	36.3	38.0	40.1	19	0.60	1.35	-0.24	-0.31	-0.32	-0.33	-0.37	-0.37	-0.35
25.0	30.9	32.6	36.2	37.9	40.0	20	0.63	1.41	-0.33	-0.39	-0.39	-0.41	-0.44	-0.44	-0.43
24.6	30.4	32.3	34.3	36.6	39.9	21	0.66	1.47	-0.41	-0.47	-0.47	-0.49	-0.51	-0.51	-0.50
23.4	30.0	30.4	34.0	36.3	36.6	22	0.69	1.54	-0.50	-0.55	-0.56	-0.57	-0.59	-0.58	-0.58
23.1	29.6	30.1	32.3	36.2	36.3	23	0.73	1.61	-0.60	-0.64	-0.64	-0.65	-0.66	-0.66	-0.65
21.7	29.4	30.0	31.3	34.8	36.2	24	0.76	1.68	-0.70	-0.73	-0.73	-0.73	-0.73	-0.73	-0.73
21.2	28.8	29.4	30.8	34.0	34.0	25	0.79	1.77	-0.80	-0.82	-0.82	-0.82	-0.80	-0.81	-0.82
21.2	25.0	28.8	30.4	31.3	31.3	26	0.82	1.86	-0.92	-0.92	-0.92	-0.92	-0.88	-0.89	-0.91
19.1	24.0	27.6	29.4	30.4	30.4	27	0.85	1.96	-1.05	-1.04	-1.03	-1.02	-0.97	-0.98	-1.00
17.5	22.7	25.0	26.4	29.4	30.4	28	0.89	2.09	-1.21	-1.16	-1.16	-1.14	-1.06	-1.08	-1.11
17.0	21.3	23.2	25.5	27.5	30.2	29	0.92	2.24	-1.39	-1.32	-1.30	-1.27	-1.17	-1.20	-1.23
15.7	17.0	21.3	23.6	26.7	27.5	30	0.95	2.46	-1.65	-1.52	-1.50	-1.45	-1.31	-1.34	-1.39
15.0	15.7	15.7	23.2	26.2	26.7	31	0.98	2.87	-2.12	-1.86	-1.83	-1.75	-1.52	-1.58	-1.65

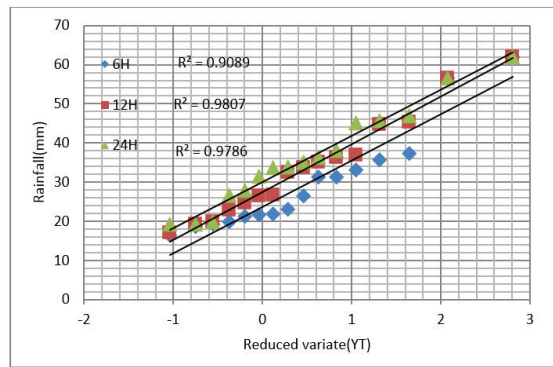
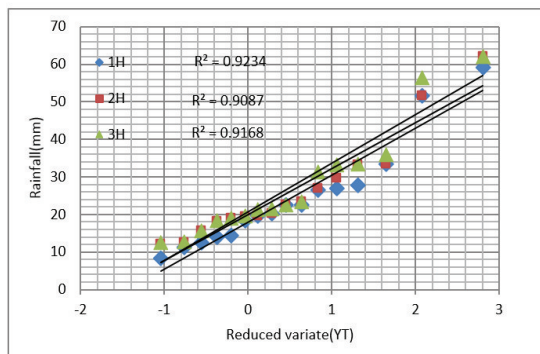


**Figure 3** Plot of reduced variate ( $Y_T$ ) against annual maximum rainfall for Gumbel EVI distribution at Lefe-isa station

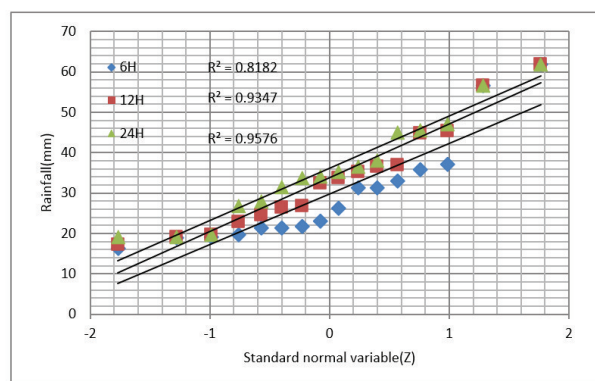
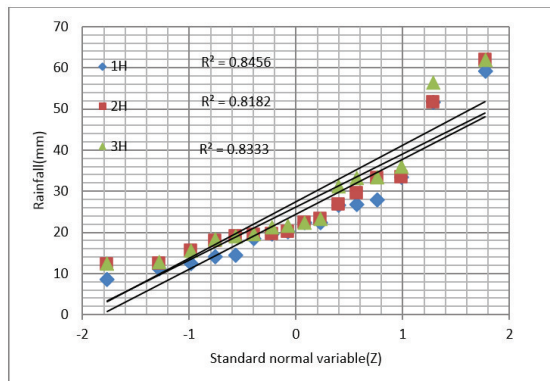


**Figure 4** Plot of standard variable ( $Z$ ) against annual maximum rainfall for Log-normal distribution at Lefe-isa station

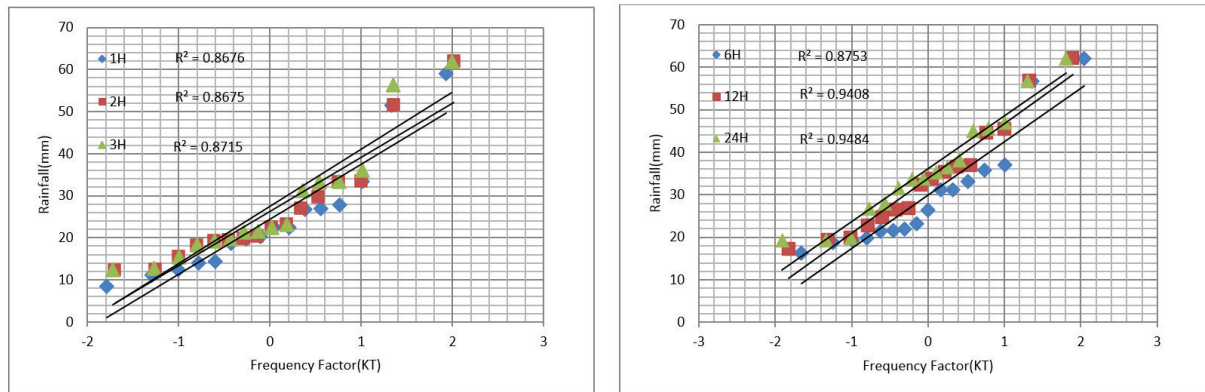


**Figure 5** Plot of frequency factor (KT) against annual maximum rainfall for Log-pearson type III distribution at Lefe-isa station

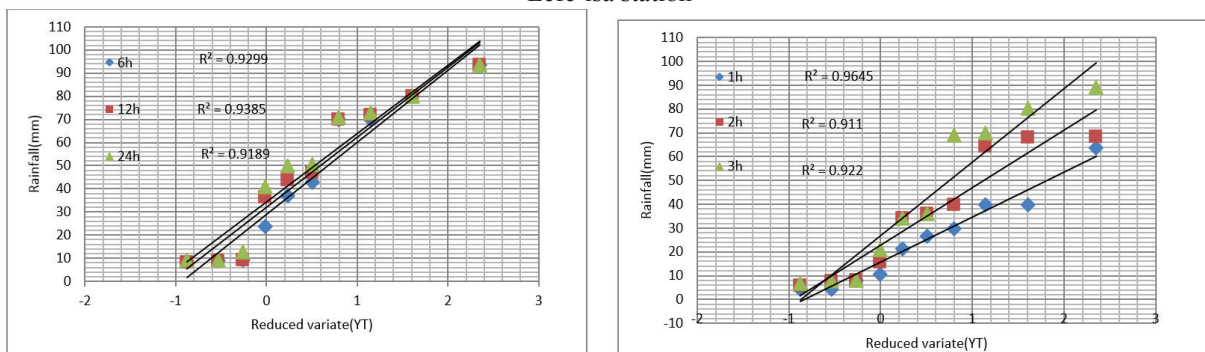


**Figure 6** Plot of reduced variate ( $Y_T$ ) against annual maximum rainfall for Gumbel EVI at Chinaksa station

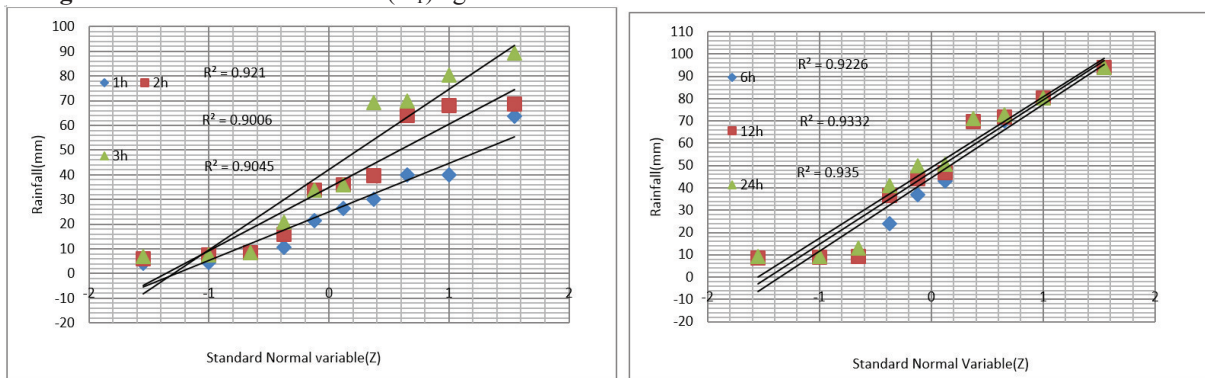


**Figure 7** Plot of Standard Normal variable (Z) against annual maximum rainfall for Log-normal at Chinaksa station

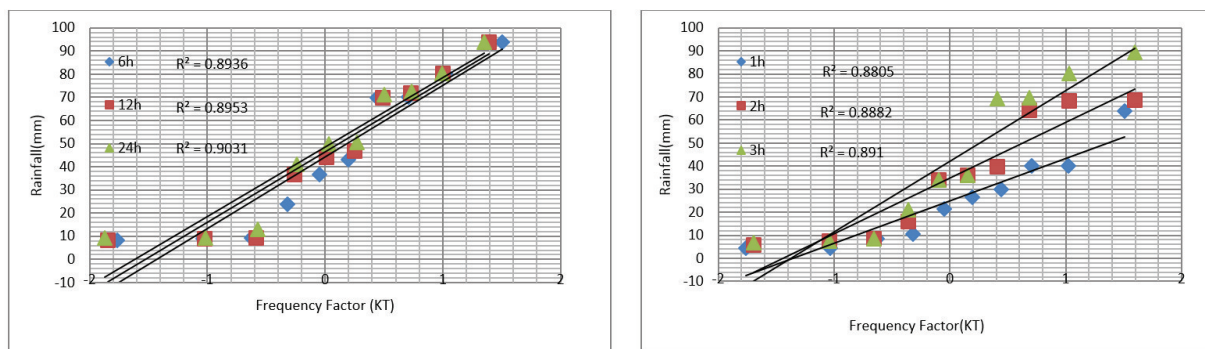


**Figure 8** Plot of frequency factor (KT) against annual maximum rainfall for Log-pearson type III at Chinaksa station

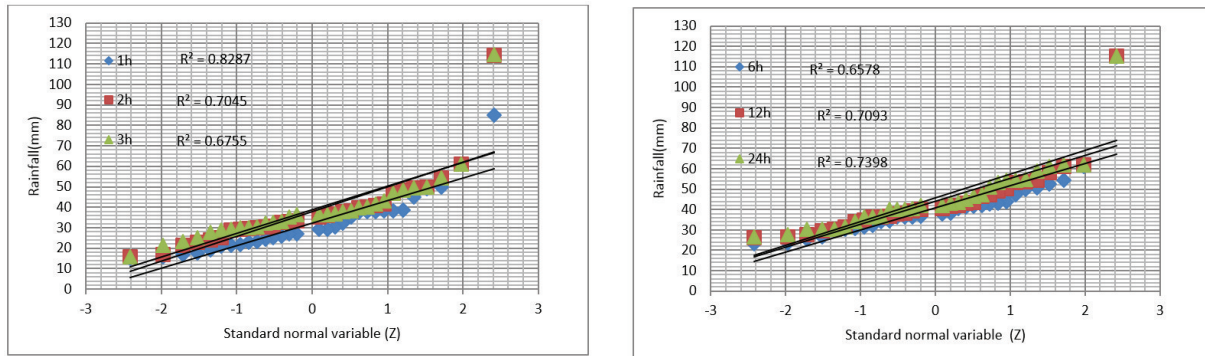


**Figure 9** Plot of reduced variate ( $Y_T$ ) against annual maximum rainfall for Gumbel EVI at Gigjiga station

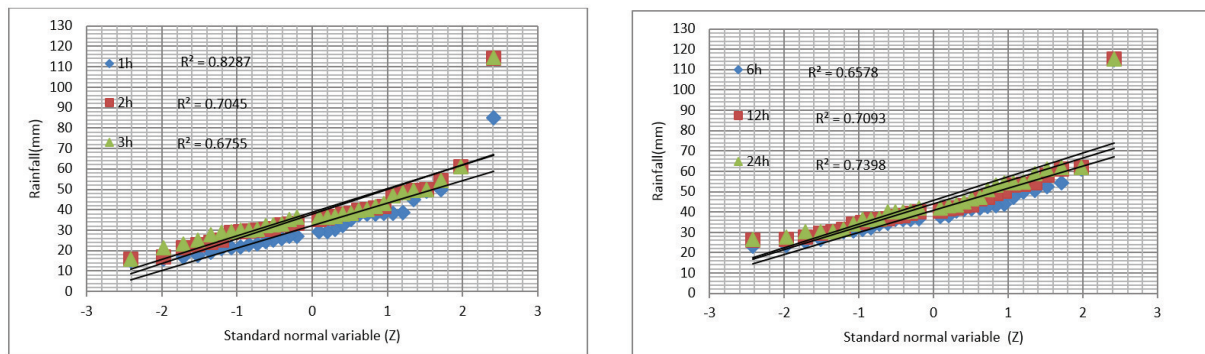


**Figure 10** Plot of Standard Normal variable ( $Z$ ) against annual maximum rainfall for Log-normal at Jigjiga station

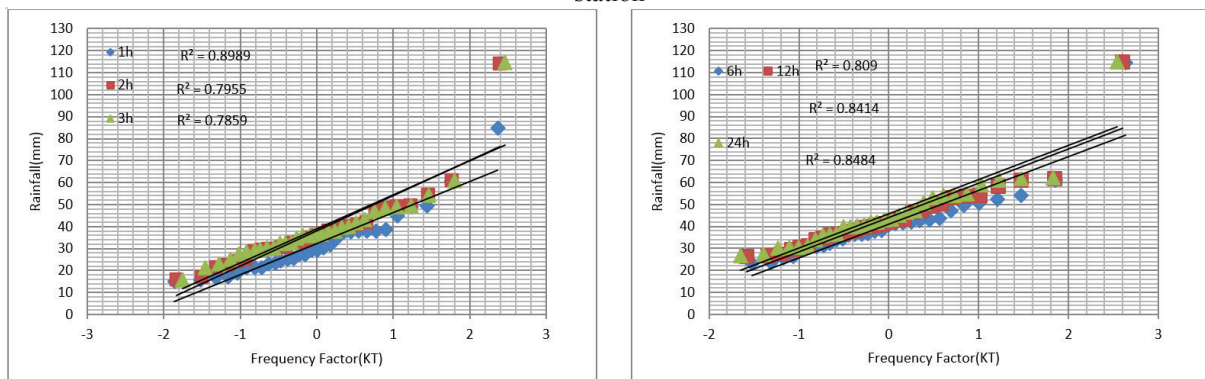


**Figure 11** Plot of frequency factor ( $KT$ ) against annual maximum rainfall for Log-pearson type III at Jigjiga station

Gumbel Extreme-Value frequency distribution is the most popular distribution and has received the highest application for estimating large events in various part of the world (Koutsoyiannis, *et al.*, 1998).

For northern and eastern part of Ethiopia, Gumbel's extreme value type I distribution was recommended to fit the annual extreme rainfall data (Cherkos *et al.*, 2006; Asres, 2008; Shemels, 2008; Ababa, 2012 and Tesfaye, 2014). However, the data series for every station was also tested for Log normal and Log Pearson Type III to check and select the best distribution function. As a result, the Gumbel probability distribution was found to be an appropriate probability distribution function that describe well the given data series for all the considered stations as indicated in Tables (2-9) and Figures (2-10).

**Table 10.** Calculated R-squared values of the probability distribution fitting test for the considered stations

Station name	Type of distribution	R-Squared values for the indicated durations (hr)							
		1H	2H	3H	6H	12H	24H	Score	Rank
Chinaksa	Gumbel	0.96	0.91	0.92	0.94	0.93	0.92		
	Log normal	0.92	0.9	0.9	0.92	0.93	0.93		
	Log Pearson	0.88	0.88	0.92	0.89	0.9	0.9	Score	Rank
	G = mark	3	3	2	3	2	2	15	1
	LN = mark	2	2	1	2	3	3	13	2
	LP = mark	1	1	3	1	1	1	8	3
Gigjiga	Gumbel	0.93	0.82	0.79	0.78	0.82	0.84		
	Log normal	0.83	0.7	0.68	0.66	0.71	0.74		
	Log Pearson	0.9	0.8	0.79	0.81	0.84	0.85	Score	Rank
	G = mark	3	3	3	2	2	2	15	1
	LN = mark	1	2	1	1	1	1	7	3
	LP = mark	2	1	2	3	3	3	14	2
Lefe-isa	Gumbel	0.92	0.91	0.92	0.91	0.98	0.98		
	Log Normal	0.85	0.82	0.83	0.82	0.93	0.96		
	Log Pearson	0.87	0.87	0.87	0.88	0.94	0.95	Score	Rank
	G = Mark	3	3	3	3	3	3	18	1
	LN =Mark	1	1	1	2	1	2	8	2
	LP = Mark	2	2	2	1	2	1	10	3

In fact, from Table 10 for the selected stations, the R-squared values for the given datasets revealed that Gumbel (EVI) probability distribution relatively better describe the maximum annual rainfall values.

### 3.2. Goodness of fit of data

The calculated and tabulated Chi-square values for the considered stations and selected duration of hours are summarized in Tables (11) and the hypothesis for the test was, if the calculated Chi-square value become greater than the tabulated  $\chi^2_{1-\alpha, v}$  at 95% confidence level with a degree of freedom ( $v=p-m-1$ ), the null hypothesis would be rejected, otherwise accepted.

**Table 11.** Calculated and tabulated Chi-square values for the considered stations at the respective duration of hours

Station name	Duration (hr)					
	1-hr		2-hr		3-hr	
	Calculated	Tabulated	Calculated	Tabulated	Calculated	Tabulated
Chinaksa	5.69	12.59	8.13	9.49	6.04	11.07
Jigjiga	10.08	19.68	18.38	22.36	19.28	22.36
Lefe-isa	5.67	15.51	7.76	15.51	8.27	14.07
	6-hr		12-hr		24-hr	
	Calculated	Tabulated	Calculated	Tabulated	Calculated	Tabulated
	Chinaksa	4.75	11.07	6.79	11.07	11.99
Jigjiga	21.61	14.07	14.34	21.03	12.44	21.03
Lefe-isa	6.93	14.07	3.08	14.07	5.00	14.07

According to Table 11, and the hypothesis made, the calculated chi-square values for all stations and the indicated durations were found to be less than the tabulated chi-square at the specified ( $\alpha=0.05$ ) significance level and degree of freedom ( $v=p-m-1$ ). Thus, Gumbel (EVI) probability distribution function was accepted to be theoretically best fitting probability distribution function for all the considered stations and duration of hours in this particular study. As a result, Gumbel (EVI) probability distribution function was adopted in this study for the computation of extreme rainfall events to construct the IDF curves.

### 3.3. Computed Extreme Rainfall Quantiles ( $X_T$ )

The computed Rainfall quartiles using the Gumbel probability distribution function for specified durations and respective return periods of the stations considered are summarized in Tables (12-14).

**Table 12.** Computed rainfall quartiles for different return periods and durations at Chinaksa station

Duration (hr)	quartiles of rainfall, $X_T$ (mm) for the indicated return periods, T(years)					
	2	5	10	25	50	100
1	22.37	45.36	60.57	79.80	94.06	108.22
2	31.41	61.65	81.67	106.96	125.73	144.35
3	37.87	76.27	101.68	133.80	157.63	181.28
6	40.06	78.46	103.88	136.00	159.83	183.49
12	42.73	80.33	105.23	136.68	160.02	183.18
24	44.88	81.74	106.14	136.97	159.84	182.54

**Table 13.** Computed rainfall quartiles for different return periods and durations at Jigjiga station

Duration (hr)	Quartiles of rainfall, $X_T$ (mm) for the indicated return periods, T(years)					
	2	5	10	25	50	100
1	29.97	44.98	54.91	67.46	76.77	86.02
2	35.17	53.22	65.17	80.27	91.47	102.59
3	36.26	53.77	65.37	80.02	90.89	101.68
6	38.37	55.17	66.29	80.34	90.77	101.12
12	41.53	58.34	69.47	83.53	93.96	104.32
24	43.13	60.01	71.19	85.31	95.78	106.18

**Table 14.** Computed rainfall quartiles for different return periods and durations at Lefe-isa station

Duration (hr)	Quartiles of rainfall, $X_T$ (mm) for the indicated return periods, T(years)					
	2	5	10	25	50	100
1	22.37	37.82	48.05	60.97	70.56	80.08
2	24.26	39.43	49.47	62.15	71.56	80.91
3	25.38	41.33	51.89	65.23	75.13	84.95
6	27.86	42.58	52.32	64.63	73.76	82.83
12	31.9	46.48	56.14	68.34	77.39	86.38
24	34.33	48.4	57.71	69.48	78.21	86.88

Generally, the computed quartiles for all rainfall durations increase in magnitude with an increase in return periods (T, years).

### 3.4. Computed Rainfall Intensities (I)

The intensities at each considered stations can be calculated by dividing the computed quartiles of the given return periods in section (3.3) to their respective durations.

### 3.5. Estimated IDF parameters

For this particular study, the ‘A’ coefficient ranges from 752.45 to 8239.25 for Lefe-isa and Jigjiga of the 2 and 100 years of return periods respectively. Whereas, The ‘B’ constant ranges from 0.21 to 101.49 for Chinaksa and Lefe-isa of the 2 and 100 years of return periods respectively. Besides, the ‘C’ exponent ranges from 0.861 to 1.19 for Lefe-isa, and chinaksa of the 2 and 100 years of recurrence interval respectively.

**Table 15.** Estimated IDF parameters using IDF Curve Fit tool for different return periods under present and future climate change scenarios at Mekelle station

RP (years)	Parameter values for the indicated return periods (T years)								
	Chineksa			Lefe-isa			Jigjiga		
	A	B	C	A	B	C	A	B	C
2	5117.28	89.70	1.082	752.45	0.206	0.861	1799.11	14.24	0.949
5	14632.50	95.58	1.143	1647.72	0.472	0.922	3430.91	17.76	0.993
10	20812.90	95.58	1.155	2288.51	0.472	0.943	4436.03	17.83	1.005
25	32321.74	101.49	1.180	3128.10	0.472	0.960	5797.91	18.33	1.017
50	37910.60	100.14	1.181	3836.51	1.090	0.972	5798.47	18.33	1.017
100	45541.99	101.49	1.187	4496.42	1.146	0.979	8239.25	20.56	1.036

From Table 15, the IDF parameters (A, B, and C) resembled to show certain trends. The “A” coefficient increases with an increase in return period for all the stations considered. The “B” constant and the “C” exponent generally increase with an increase in “A” coefficient.

### 3.6. Mathematical Expressions of the IDF Curves

IDF relationship can be expressed in the form of empirical equations rather than reading the rainfall intensity

from graphs or maps. Hence a mathematical expression was developed for the considered stations to compute extreme rainfall intensities exceeding the observed data using the estimated IDF parameters for a given duration and frequency with a general form given by EXACT (2006):

$$I = \exp[(\ln A - C \ln(B + D))] \quad (3.1)$$

Where, A, B and C are the estimated IDF parameters and D is time duration in minutes.

Concurrently, each station had different equations for different return periods. The resulting six equations for each station were used for intensity calculations in the area represented by that station. Therefore, six equations for the return periods of 2, 5, 10, 25, 50, and 100 years are listed for the IDF relationships of the considered stations in Table 16.

**Table 16.** Mathematical IDF equations for the considered stations at different return periods

Station name	Return period	Mathematical Expressions
Chinaksa	2	$I = \exp[(\ln 5117.28 - 1.082 \ln(89.7 + D))]$
	5	$I = \exp[(\ln 14632.5 - 1.143 \ln(95.58 + D))]$
	10	$I = \exp[(\ln 20812.9 - 1.155 \ln(95.58 + D))]$
	25	$I = \exp[(\ln 32321.74 - 1.18 \ln(101.49 + D))]$
	50	$I = \exp[(\ln 37910.6 - 1.181 \ln(100.14 + D))]$
	100	$I = \exp[(\ln 45541.99 - 1.187 \ln(101.49 + D))]$
Jigjiga	2	$I = \exp[(\ln 1799.11 - 0.949 \ln(14.24 + D))]$
	5	$I = \exp[(\ln 3430.91 - 0.993 \ln(17.76 + D))]$
	10	$I = \exp[(\ln 4436.03 - 1.005 \ln(17.83 + D))]$
	25	$I = \exp[(\ln 5797.91 - 1.017 \ln(18.33 + D))]$
	50	$I = \exp[(\ln 5798.47 - 1.017 \ln(18.33 + D))]$
	100	$I = \exp[(\ln 8239.25 - 1.036 \ln(20.56 + D))]$
Lefe-isa	2	$I = \exp[(\ln 752 - 0.861 \ln(0.206 + D))]$
	5	$I = \exp[(\ln 1647.72 - 0.922 \ln(0.472 + D))]$
	10	$I = \exp[(\ln 2288.51 - 0.943 \ln(0.472 + D))]$
	25	$I = \exp[(\ln 3128.10 - 0.960 \ln(0.472 + D))]$
	50	$I = \exp[(\ln 3836.51 - 0.972 \ln(1.090 + D))]$
	100	$I = \exp[(\ln 4496.42 - 0.979 \ln(1.146 + D))]$

Based on the above developed equations, intensity values were computed for the respective stations at different return periods and are summarized in Tables (17-19).

**Table 17.** Computed intensity of rainfall, I (mm/hr) using the IDF parameters at Chinaksa station

Duration (hr)	Intensity of rainfall, I (mm/hr) for the indicated return period, T(years)					
	2	5	10	25	50	100
1	22.66	45.76	61.17	80.13	94.61	108.73
2	15.74	31.52	41.96	55.19	64.98	74.71
3	11.99	23.81	31.6	41.59	48.89	56.21
6	6.89	13.4	17.68	23.21	27.21	31.25
12	3.65	6.89	9.02	11.75	13.75	15.76
24	1.83	3.34	4.35	5.59	6.54	7.46

**Table 18.** Computed intensity of rainfall, I (mm/hr) using the IDF parameters at Jigjiga station

Duration (hr)	Intensity of rainfall, I (mm/hr) for the indicated return period, T(years)					
	2	5	10	25	50	100
1	30.21	45.45	55.73	68.64	68.64	87.34
2	17.22	25.76	31.38	38.48	38.49	49.07
3	12.13	17.99	21.82	26.67	26.68	33.95
6	6.51	9.46	11.39	13.83	13.83	17.49
12	3.43	4.87	5.81	7	7	8.77
24	1.8	2.47	2.93	3.5	3.5	4.34

**Table 19.** Computed intensity of rainfall, I (mm/hr) using the IDF parameters at Lefe-isa station

Duration (hr)	Intensity of rainfall, I (mm/hr) for the indicated return period, T(years)					
	2	5	10	25	50	100
1	22.06	37.52	47.84	60.9	70.45	80.05
2	12.16	19.88	24.98	31.42	36.23	40.98
3	8.58	13.69	17.06	21.31	24.5	27.63
6	4.73	7.24	8.89	10.97	12.53	14.06
12	2.6	3.82	4.63	5.64	6.39	7.14
24	1.43	2.02	2.41	2.9	3.26	3.63

As shown in Tables (17-19), highest intensity of rainfall (30.219 mm/hr) for 2 years recurrence interval within 1-hr duration was observed at Jigjiga station while the lowest (22.06 mm/hr) was observed at Lefe-isa station. Besides, the daily maximum intensity of rainfall was found to be highest (1.83mm/hr) at Chinaksa station while the lowest one (1.43 mm/hr) was for Lefe-isa station.

On the other hand, among the considered stations, the highest rainfall intensity (108.73mm/hr) at 1-hr duration is likely to occur at Chinaksa station and relatively the smallest (80.05mm/hr) intensity of rainfall will occur at Lefe-isa station for 100 years of recurrence interval.

### 3.7. Sensitivity of the IDF Parameters

From the sensitivity test of the IDF parameters, it was observed that the “C” exponent was found to be the most sensitive parameter. An increase in “C” exponent by 10% resulted in a difference of 41.84 to 54.81% between the intensity of rainfall obtained by the optimized and the increased parameters. This is a good indication that care has to be taken in determining the “C” exponent. Increasing the “A” coefficient by 10% resulted in a slight decrease on the intensity by approximately 10% which indicates that the rate of increase or decrease in “A” coefficient causes a slight decrease or increase of the intensity of rainfall. An increase in the “B” constant had no shown significant change on the intensity of rainfall

Table (20) presents the results of the sensitivity test on the IDF parameters for a return period of 2 years at Chinaksa station using the following equation from Table 16:  $I = \exp [(\ln 5117.28 - 1.082 \ln (89.7 + D))]$  where, I is intensity of rainfall at a given duration and D is duration in minutes.

**Table 20** Comparison of the intensity of rainfall obtained from the optimized and the increased parameters at Chinaksa station

Duration (hours)	I, with optimized (A, B and C)	I, with 10% increase in (A)	I, with 10% increase in (C)	I, with 10% increase in (B)	% change at (A)	% change at (C)	% change at (B)
1	22.66	24.93	13.18	21.28	-10.00	41.84	6.10
2	15.27	16.80	8.54	15.04	-10.00	44.09	1.53
3	11.71	12.88	6.38	11.57	-10.00	45.56	1.20
6	6.70	7.37	3.45	6.75	-10.00	48.51	-0.66
12	3.60	3.96	1.74	3.61	-10.00	51.62	-0.19
24	1.82	2.00	0.82	1.82	-10.00	54.81	-0.20

### 4.8. Test for Model Performance

The resulting,  $R^2$  and  $E_{NS}$  values for the IDF model performance evaluation for the given return periods with respective durations of the data sets are summarized in Table (4.21) for all the considered stations

**Table 21.** Values of regression coefficient ( $R^2$ ) and Nash-Sutcliffe simulation efficiency ( $E_{NS}$ ) between the observed and estimated rainfall intensities

Station Name	$R^2$ values for indicated frequencies, T(years)						$E_{NS}$ values for indicated frequencies, T (years)					
	2	5	10	25	50	100	2	5	10	25	50	100
Chinaksa	0.998	0.997	0.997	0.997	0.997	0.997	0.9983	0.9974	0.9969	0.9969	0.9966	0.9966
Jigjiga	1	0.999	0.999	0.999	0.999	0.999	0.9996	0.9992	0.9988	0.9985	0.9985	0.9985
Lefe-isa	1	1	1	1	1	1	0.9996	0.9998	0.9999	0.9999	0.9998	0.9998

$R^2$  and  $E_{NS}$  can range from 0 to 1 and  $-\infty$  to 1 respectively. The closer the  $R^2$  to 1, the better the regression equation fits the data and an efficiency of 1 indicates a perfect match between observed and estimated intensities (Moriassi *et al.*, 2007).

As shown in Table (21), the ( $R^2$ ) and  $E_{NS}$  values were found to be very close to 1. This depicts that there were good direct correlations between the observed and estimated intensities. Hence, it can be said that the computed intensity values obtained by using the IDF parameters would adequately describe the observed data and the parameter estimation model performs very well. Therefore, using the computed rainfall intensity values



of different durations and return periods, the IDF curves for the selected stations were constructed.

#### 4.9. Construction of IDF Curves

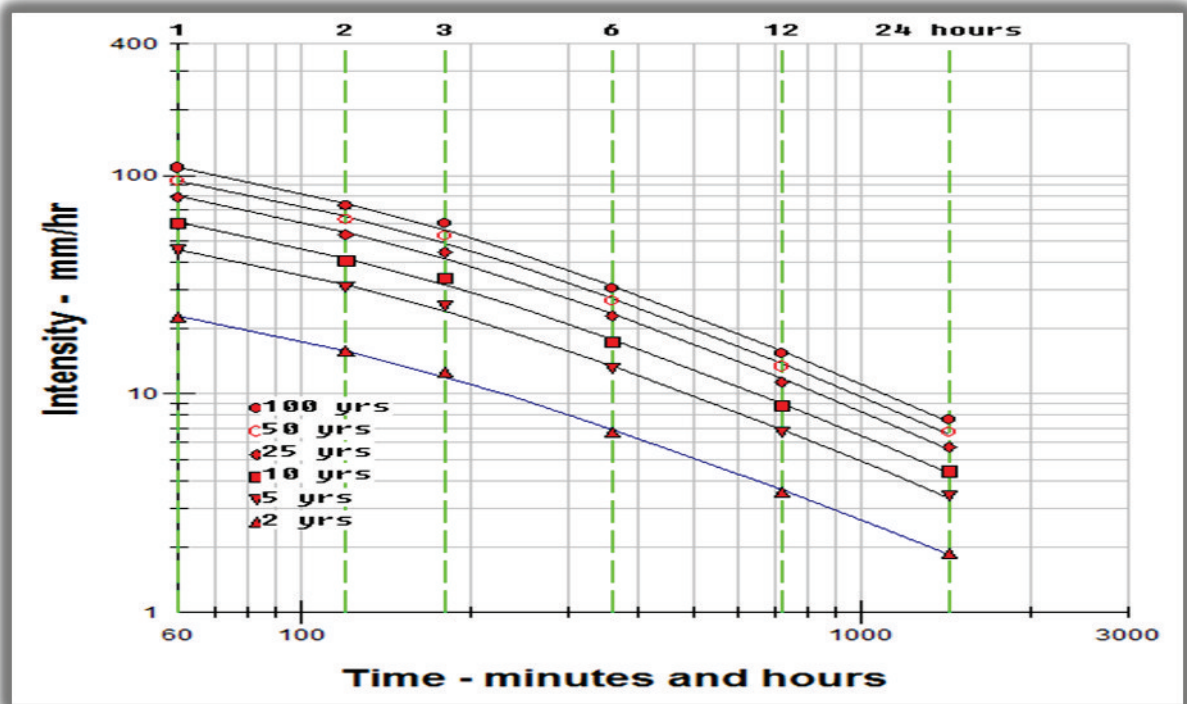


Figure 12 IDF curve for Chinaksa station

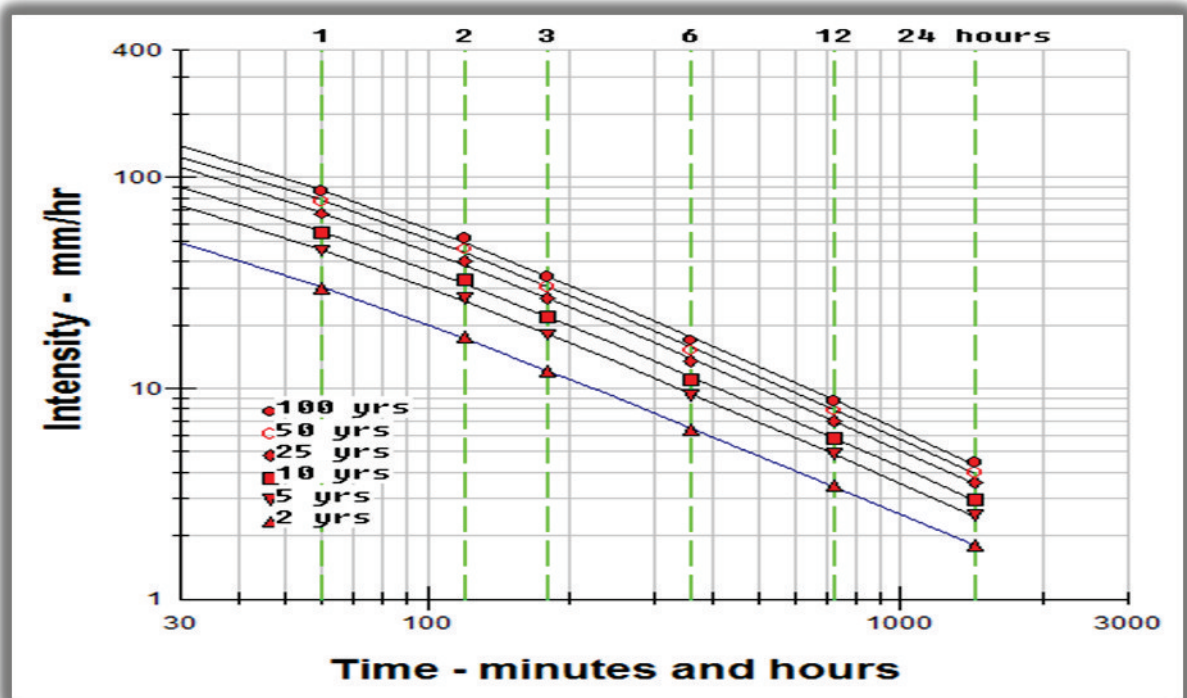


Figure 13 IDF curve for Jigjiga Station

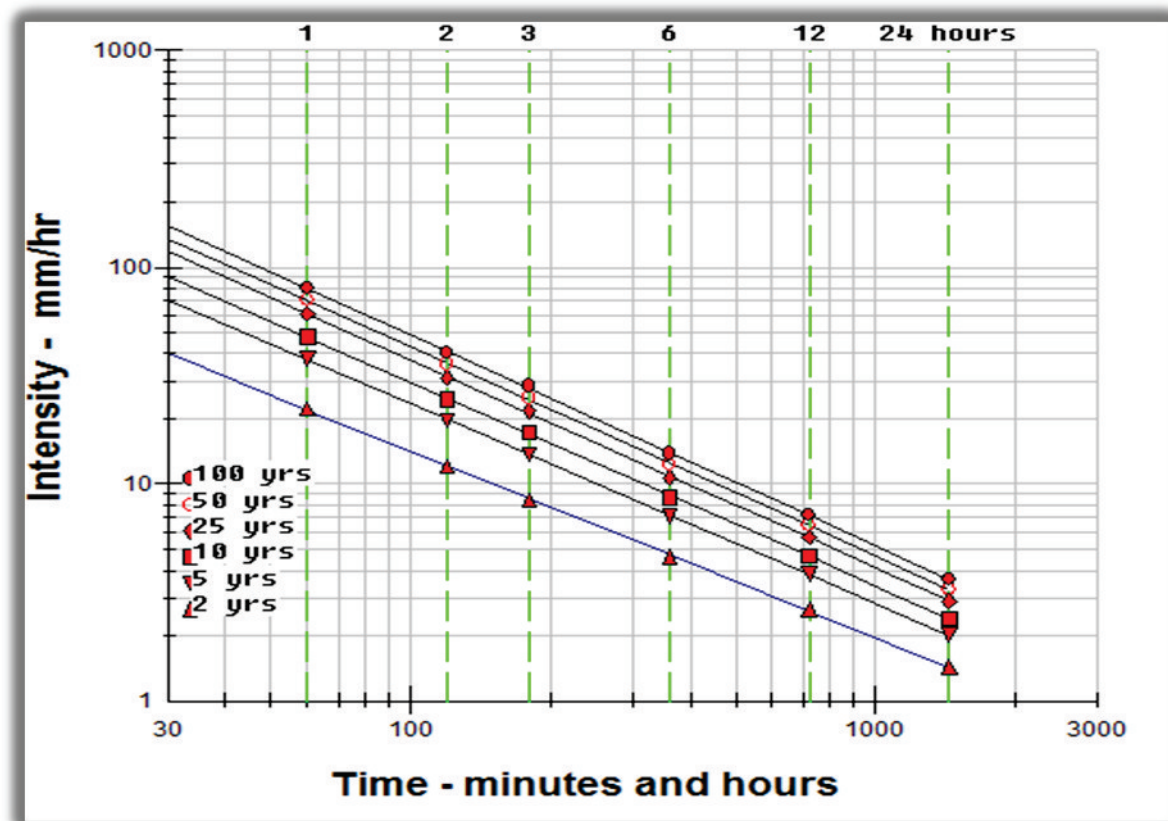


Figure 14 IDF curve for Lefe-isa station

## 5. CONCLUSIONS

Intensity-Duration-Frequency (IDF) relationship is one of the most critical tools used in the development of water resource systems and drainage works. The availability of a number of rainfall recording stations in the nation increased. Consequently it is possible to develop IDF relationships for different stations, regions and in the longrun for the country. Hence, in this research, an attempt was made to determine the curve coefficients (a, b and c) required to develop IDF curves and estimating the rainfall depth/intensities using MIDDUS computer program for return periods of 2, 5, 10, 25, 50 and 100 years and for all durations for the selected meteorological stations in the Ethiopian Somali region. Finally the following conclusions were drawn from the research work:

- ☞ Based on the goodness of fit among the three common probability distributions functions (i.e. Log-normal, Log-Pearson and Gumbel EVI), Gumbel EVI probability distribution is the best model to fit the historical or observed data for the selected stations in the study area.
- ☞ The IDF curve fit parameters (A, B and C) generated with a software known as MIDUSS show an increasing or decreasing trend with an increase or decrease in return period. Generally, the parameters vary from 752 to 8239.3 for 'A', 0.21 to 101.49 for 'B' and 0.86 to 1.19 for parameter 'C'.
- ☞ The IDF parameter estimation model was evaluated its performance by determining the coefficient of determination (R-sq) and Nush suchlif simulation efficiency between the Observed intensities and computed intensities by the IDF parameters. Since the R-sq and  $E_{NS}$  was very high, over 0.99, that depicts a strong relation between the observed and computed intensities. Hence, the developed IDF parameters can be used as a useful tool for the estimation of the rainfall design parameters for water resource development and similar works. Thus, the results obtained serve to meet the need for rainfall IDF relationships for the selected stations in the Ethiopian Somali Region.
- ☞ The IDF curve developed and the IDF parameters generated for the return periods of 2, 5, 10, 25, 50 and 100 years for all durations are good to use for water resource designing, soil and water conservation practices, etc. Hence, the need of these values has been particularly great because there is no similar work done for the study area.

## Acknowledgements

My deepest and unreserved thanks also go to Jigjiga University for financial support. Thanks are also to Ethiopian National Meteorology Service Agency Addis Ababa head office and Ethiopia Somali region jigjiga

branch, for their affordance of meteorological data.

Finally, I express my sincere thanks to all individuals who provided fruitful suggestions and helped me in different ways to accomplish the work successfully.

#### 4. REFERENCES

- [1] Chow, V.T, Maidment, D.R., and Mays, L.W. (1988). Applied Hydrology McGraw-Hill Book Company, Singapore.
- [2] IPCC (2007). J.H. Christensen, B. Hewitson, A. Busuioc, A. Chen, X. Gao, I. Held, R. Jones, R.K. Kolli, W.-T. Kwon, R. Laprise, V. Magaña Rueda, L. Mearns, C.G. Menéndez, J. Räisänen, A. Rinke, A. Sarr, and P. Whetton. Climate Change 2007: The Physical Science Basis. Contribution of Working Group I to the Fourth Assessment Report of the Intergovernmental Panel on Climate Change, chapter 11: Regional Climate Projections. Cambridge University Press, Cambridge, United Kingdom and New York, NY, USA, 2007.
- [3] IPCC 2007. M.L. Parry, O.F. Canziani, J.P. Palutikof, P.J. van der Linden, and C.E. Hanson, editors. Climate Change 2007: Impacts, Adaptation and Vulnerability. Contribution of Working Group II to the Fourth Assessment Report of the Intergovernmental Panel on Climate Change, chapter Summary for Policymakers. Cambridge University Press, Cambridge, United Kingdom and New York, NY, USA.
- [4] IPCC 2007. S. Solomon, D. Qin, M. Manning, Z. Chen, M. Marquis, K.B. Averyt, M.Tignor, and H.L. Miller, editors. Climate Change 2007: The Physical Science Basis. Contribution of Working Group I to the Fourth Assessment Report of the Intergovernmental Panel on Climate Change, chapter Summary for Policymakers. Cambridge University Press, Cambridge, United Kingdom and New York, NY, USA.
- [5] Mailhot, A. and Duchesne, S. (2010). Design criteria of urban drainage infrastructures under climate change, *Water Resource Plan Management* 136, 201–208.
- [6] MTO (1997). Ministry of Transportation of Ontario Drainage Management Manual. Drainage and Hydrology Section, Transportation Engineering Branch, and Quality Standards Division, Ministry of Transportation of Ontario, Ottawa, Ontario, Canada.
- [7] Nakicenovic, N. and Swart, R. (2000). IPCC Special Report on Emissions Scenarios, Intergovernmental Panel on Climate Change. Cambridge University Press, Cambridge, United Kingdom.
- [8] Slobodan P. Simonovic and Angela Peck (2010). Updated rainfall intensity duration frequency curves for the City of London under the changing climate. Department of Civil and Environmental Engineering, the University of Western Ontario London, Ontario, Canada, p 1-19.
- [9] USACE (2000). Hydrologic Modeling System HEC-HMS, Technical reference manual. United States Army Corps of Engineers, Hydrologic Engineering Center, Davis, California.